

Adaptive Digital Feedback Predistortion Technique for Linearizing Power Amplifiers

Young Yun Woo, Jangheon Kim, Jaehyok Yi, Sungchul Hong, Ildu Kim, Junghwan Moon, and Bumman Kim, *Fellow, IEEE*

Abstract—We have developed a new adaptive digital predistortion (DPD) linearization technique based on analog feedback predistortion (FBPD). The lookup-table-based feedback input can remove the bandwidth limitation of the feedback circuit related to the loop delay, and suppress feedback oscillation by accurate digital control of the feedback signal. Moreover, the predistortion (PD) signal can be extracted very efficiently. By combining the feedback linearization and DPD linearization techniques, the performance of the predistorter is enhanced significantly compared to the conventional DPD. To clearly visualize the characteristics of digital FBPD (DFBPD), we have compared it to the conventional DPD based on the recursive least square algorithm using MATLAB simulation. The results clearly show that the new method is a good linearization algorithm, better than a conventional DPD. For the demonstration, a Doherty power amplifier with 180-W peak envelope power is linearized using the proposed DFBPD. For a 2.14-GHz forward-link wideband code-division multiple-access signal, the adjacent channel leakage ratio at 2.5-MHz offset is -58 dBc, which is improved by 15 dB at an average output power of 43 dBm.

Index Terms—Digital feedback predistortion (DFBPD), digital predistortion (DPD), feedback predistortion (FBPD), linearization, lookup table (LUT), power amplifier (PA), quantization, recursive least square (RLS), wideband code division multiple access (WCDMA).

I. INTRODUCTION

CURRENT wireless communication systems, such as code division multiple access (CDMA)-2000, wideband code division multiple access (WCDMA), orthogonal frequency division multiplex (OFDM), etc., transmit nonconstant envelope signals to efficiently use the limited frequency resource. These

Manuscript received November 29, 2006; revised February 3, 2007. This work was supported in part by the Korean Ministry of Education under the BK21 Project and by the Center for Broadband Orthogonal Frequency Division Multiplex Mobile Access, Pohang University of Science and Technology under the Information Technology Research Center Program of the Korean Ministry of Information Technology, supervised by the Institute for Information Technology Advancement (IITA-2006-C1090-0603-0037).

Y. Y. Woo and S. Hong are with the Telecommunication Research and Development Center, Samsung Electronics Company Ltd., Suwon, Gyeonggi 442-742, Korea (e-mail: w.yun@postech.ac.kr).

J. Kim, I. Kim, J. Moon, and B. Kim are with the Department of Electrical Engineering, Pohang University of Science and Technology, Pohang, Gyeongbuk 790-784, Korea (e-mail: bmkim@postech.ac.kr; rage3k@postech.ac.kr).

J. Yi is with the Mobile Handset Research and Development Center, Telecommunication Equipment and Handset Company, LG Electronics Inc., Seoul 153-801, Korea.

Color versions of one or more of the figures in this paper are available online at <http://ieeexplore.ieee.org>.

Digital Object Identifier 10.1109/TMTT.2007.895145

modulated signals vary rapidly and have high peak-to-average ratio (PAR). The power amplifiers (PAs) for these systems require high linearity to amplify the signals without distortion. However, due to the high PAR, the PAs operate at a large backoff power level to achieve the linearity and, therefore, have low efficiency. In order to increase the efficiency, the PAs have been operated at a higher power level and various linearization techniques, such as feedback, analog predistortion (PD), and feed-forward, have been adopted to enhance the linearity [1]–[7]. It is difficult to employ these RF linearization techniques as a complete transmitter for a base station due to the complicated circuits and/or insufficient linearization.

A promising technique to remove the drawbacks of the RF linearization technique is, undoubtedly, digital predistortion (DPD) using a digital signal processor (DSP). The DPD based on error feedback correction is a powerful linearization technique because it has the nature of a manageable digital operation, and the error correction is insensitive to amplifier variations, such as temperature, supply voltage, and device variations, as well as nonlinear characteristics of the PA. Among the DPD linearization techniques, the lookup table (LUT)-based DPD has been widely used because it is relatively simple and easily implemented to build the inverse function of PAs [8]–[15]. In the PD algorithms that provide as the inverse function of the amplitude and phase distortions (AM/AM and AM/PM) generated by the PAs, the basic and most important issue is that the estimation error, the difference between the desired and the estimated values, should reach the minimum value for a given input signal. This value can be obtained by applying successive iterations to minimize the estimation error using least mean square (LMS) or recursive least square (RLS) in direct or indirect architectures [14], [15].

In this paper, we propose a new digital adaptive PD technique by employing analog feedback predistortion (FBPD) theory in the digital domain. The analog FBPD linearization method can accurately extract the PD signal and enhance the tolerance of the intermodulation (IM) distortion cancellation by the feedback linearization, as reported by our group [16]. The critical problems of FBPD are the operation at bandwidth limitation caused by the loop delay, and an oscillation tendency caused by the feedback nature. By employing a digital LUT technique, these limitations can be overcome, while maintaining the advantages of the feedback circuit. Moreover, FBPD can enjoy the abundant merits of the DPD. In the linearizer, the main signal, as well as the error, are fed back, suppressing the open loop gain. We believe that this is the first report of PA linearization using PD and feedback techniques together in the digital domain, which

eliminates the problems of the RF feedback circuit. As a result, the distortion correction of the PD is carried out by the DPD and further enhanced by the feedback linearization. Compared to conventional DPD, the IM cancellation tolerance is enhanced by a factor of the gain compression of the feedback circuit, and the error extraction algorithm is very simple.

The remainder of this paper is organized as follows. Section II describes the DFBPD architecture and algorithm based on the RF FBPD theory. In Section III, we present a full analysis of the linearization performance and tolerance of the DFBPD technique using MATLAB simulation. This includes: 1) convergence behavior; 2) system tolerance; 3) effects of detector errors; 4) modulator errors; 5) loop delay mismatches; and 6) analysis of quantization errors with various bit widths. To clearly visualize the characteristics of the DFBPD, we have compared it to conventional DPD based on the RLS algorithm using a single-carrier WCDMA signal. In Section IV, we have experimentally verified that DFBPD is a good linearization technique, and explored some of its important characteristics. Finally, conclusions are drawn in Section V.

II. OPERATION OF DFBPD

A. FBPD Technique

Fig. 1(a) shows a simplified block diagram of the RF FBPD presented in [16]. The system consists of three blocks, i.e., “feeding block,” “cancelling block,” and “main amplifier block.” In the cancelling block, the error signal of the amplifier, $e(t)$ is extracted from the main amplifier output, $y(t)$ by eliminating the estimated input signal component to the amplifier $u(t)$. The PD signal, which is suitable for linearizing the main amplifier is extracted. The predistorted signal is fed back to the input of the main amplifier by the feeding block. The cancelling loop is similar to the feedforward main signal cancelling loop. In the frequency domain, the input signal X , the predistorted signal U , the PD signal E , the distortion of the amplifier X_d , the error of the detection loop X_f , and the output signal Y of the FBPD system are expressed as

$$\begin{aligned} U &= X + E \\ E &= G_u \cdot U - G_y \cdot Y - X_f \\ Y &= G_m \cdot U + X_d \end{aligned} \quad (1)$$

where G_u is the complex signal gain of the cancellation block, G_m is the complex signal gain (open loop) gain of the main forward path, and G_y is the complex signal gain of the feedback path, as shown in Fig. 1(a). The capital letters denote frequency-domain representation of each signal.

From the above equations, U and Y are given by

$$\begin{aligned} U &= \frac{X}{(1 - G_u) + G_y \cdot G_m} - \frac{G_y \cdot X_d}{(1 - G_u) + G_y \cdot G_m} \\ &\quad + \frac{X_f}{(1 - G_u) + G_y \cdot G_m} \end{aligned} \quad (2)$$

$$\begin{aligned} Y &= \frac{X}{(1 - G_u)/G_m + G_y} + \frac{(1 - G_u) \cdot X_d}{(1 - G_u) + G_y \cdot G_m} \\ &\quad + \frac{X_f}{(1 - G_u)/G_m + G_y} \end{aligned} \quad (3)$$

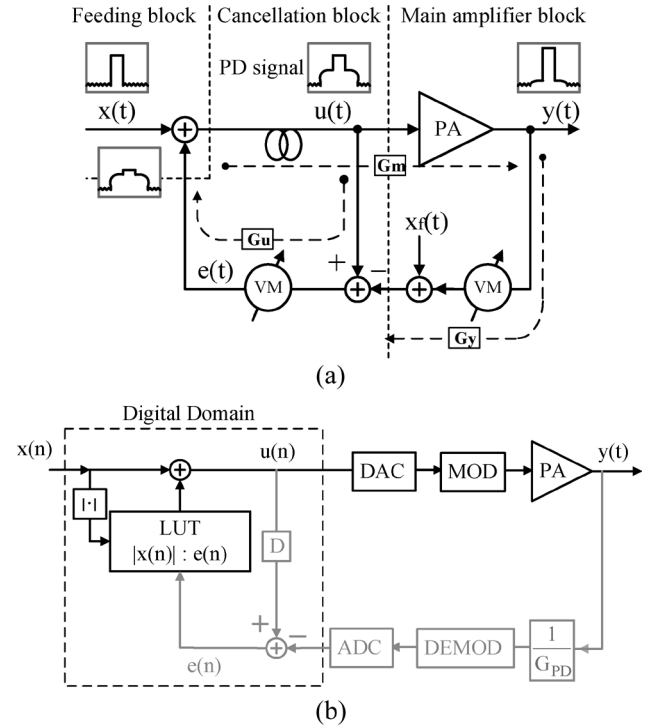


Fig. 1. Simplified block diagrams of: (a) analog feedback predistorter and (b) digital feedback predistorter.

$$\approx \frac{X}{G_y} + \frac{(1 - G_u) \cdot X_d}{G_y \cdot G_m} + \frac{X_f}{G_y}. \quad (4)$$

In (2)–(4), the first term is the fundamental signal amplification, the second term is the IM signal cancellation, and the third term is the feedback loop distortion. The approximation (4) clearly shows the feedback operation of the system; the overall gain of the FBPD, G_{PD} is determined by the feedback loop gain only, i.e., $1/G_y$, which is independent of the amplifier gain fluctuation due to temperature variation, etc. The $(1 - G_u)$ term indicates that the PD signal is extracted from the loop and is injected into the main amplifier. For accurate PD, G_u should be adjusted close to the 1. The IM component is further suppressed by a factor of closed loop gain $G_y \cdot G_m$ due to the negative feedback operation. Therefore, the system is called FBPD. However, the detector circuit error X_f is forwarded to the output, and significant improvements of the error are not effected compared to the conventional DPD algorithm.

The structure of the proposed DFBPD, shown in Fig. 1(b), is the same as analog feedback, except that the feedback signal $e(t)$ in the cancellation loop constructs a LUT in the digital domain, and the gain factors G_u and G_y of the signal cancelling and feedback paths are adjusted by the DSP instead of using vector modulators (VMs) in the RF domain. The PD signal is extracted directly from the LUT, which has been updated using the error signal extracted at the signal cancellation loop beforehand. Thus, the time delay through the loop is eliminated, and the bandwidth limitation does not exist. The oscillation tendency of the feedback circuit can be suppressed easily by digital control of the feedback component. Moreover, the abundant advantages of the FBPD circuit mentioned above can be utilized for

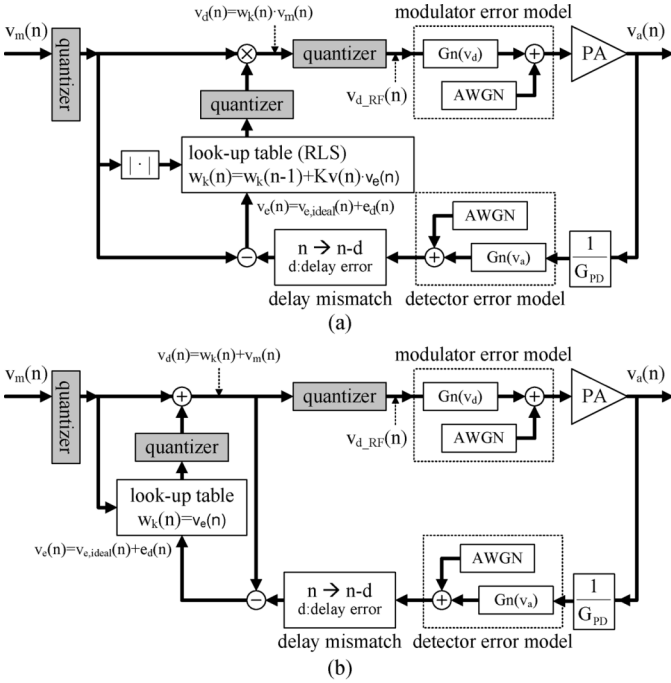


Fig. 2. Equivalent structures of: (a) conventional DPD and (b) DFBDP linearizers.

the linearization. The distortion correction of the PD is carried out by the DPD and further enhanced by the feedback linearization. Another merit of the DFBDP is rapid convergence due to efficient PD signal extraction by the feedback circuit, and the initial condition for the PD signal has little effect on the convergence behavior. To validate the expected performances of the DFBDP, we have compared it to the conventional PD using extensive simulations, which will be presented in Section II-B.

B. Equivalent Models and Adaptive Algorithms

Fig. 2(a) and (b) shows the equivalent models of the conventional DPD and proposed DFBDP. Each model includes several error models for the detector, a modulator, a delay mismatch block, a PD signal error, and quantizer blocks to test performance and check tolerances under various conditions. As shown in Fig. 2, the additive white Gaussian noise (AWGN) and third-order nonlinear elements $Gn(\cdot)$ are used as error sources for the detection and modulation parts, modeling the thermal noise and mixer nonlinearity, respectively. The delay mismatch blocks are added to represent the overall loop delay mismatches. The quantizer blocks are also included to analyze the quantization errors of the source signal, LUT, and PD output.

The DPD employs the RLS adaptive algorithm to extract the error signal to provide fast convergence [17]. The extracted error signal is stored into a LUT, and a stored value multiplies the input signal to generate a PD signal. For the FBDP, we can directly extract an accurate error from the feedback loop (cancellation loop), and the error signal is stored into the LUT. The stored error signal is then added to the input as a PD signal without any loop delay.

The PD signal generation and the adaptation algorithms of the DFBDP are quite different from the conventional DPD. The

RLS adaptive algorithm is initialized by

$$\hat{W}(0) = [1 \ 1 \ 1 \ \dots \ 1 \ 1]^T \quad (5)$$

$$P(0) = \delta^{-1}I \quad (6)$$

where δ is a small positive constant, $\hat{W}(0)$ is a $K \times 1$ vector, where K is the size of the LUT, and I is the $K \times K$ identity matrix. Next, for each time, $n = 1, 2, \dots$, computed as

$$\pi(n) = P(n-1)v_m(n) \quad (7)$$

$$K_v(n) = \frac{\pi(n)}{\lambda + v_m^H(n)\pi(n)} \quad (8)$$

$$v_e(n) = v_m(n) - \frac{v_a(n)}{G_{PD}} \quad (9)$$

$$\hat{W}(n) = \hat{W}(n-1) + K_v(n)v_e^*(n) \quad (10)$$

$$P(n) = \lambda^{-1}P(n-1) - \lambda^{-1}K_v(n)v_m^H(n)P(n-1) \quad (11)$$

where λ is the forgetting factor (a scalar value) and $P(n)$ is a $K \times K$ matrix. Both $\pi(n)$ and $K_v(n)$ are the $K \times 1$ matrices. The LUT is constructed and updated by each successive iteration. On the other hand, the DFBDP algorithm is very simple and expressed as

$$\hat{W}(n) = v_e(n-1) = v_d(n-1) - \frac{v_a(n-1)}{G_{PD}}, \quad n = 1, 2, 3, \dots \quad (12)$$

where $v_d(n)$ is the predistorted input signal, $v_a(n)$ is the final output signal, and G_{PD} is the overall PD system gain. The LUT is constructed by this error signal $v_e(n)$.

III. SIMULATION RESULTS

We have carried out system simulations based on the equivalent models to evaluate the linearization performance of the PDs using MATLAB simulation. The nonlinear PA is modeled from the AM/AM and AM/PM conversion of a Freescale 21030 LDMOS amplifier using a fifth-order polynomial function. The AM/AM conversion gain G_m and the PD system gain G_{PD} are adjusted to 44.2 and 42.25 dB, respectively, which is approximately 2-dB gain suppression by the feedback loop. The modulated input signal is a single-carrier forward WCDMA signal with a 3.84-MHz chip rate and 9.8-dB PAR at a 0.01% complementary cumulative distribution function (CCDF), which is generated by using the 3GPP WCDMA library of Agilent's Advanced Design System (ADS). A monotonically increasing signal from the minimum to maximum range of the input signal is used as a training sequence to find the optimum PD LUT.

A. Convergence Behavior

Convergence tests for the DFBDP and DPD are carried out for an ideal case with no system error. Fig. 3(a) shows the residual output error as a function of the number of iterations for each algorithm, showing much fast convergence for the DFBDP. Only eight iterations are sufficient for the DFBDP to suppress the spectral regrowth of the amplifier to the source signal level, while approximately 30 iterations are required for the conventional DPD. Fig. 3(b) shows the power spectral densities (PSDs) of the output signals and residual errors of the DPD and DFBDP

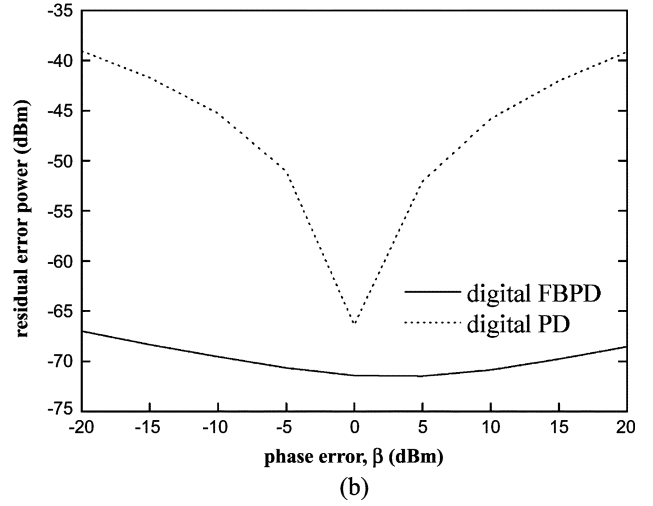
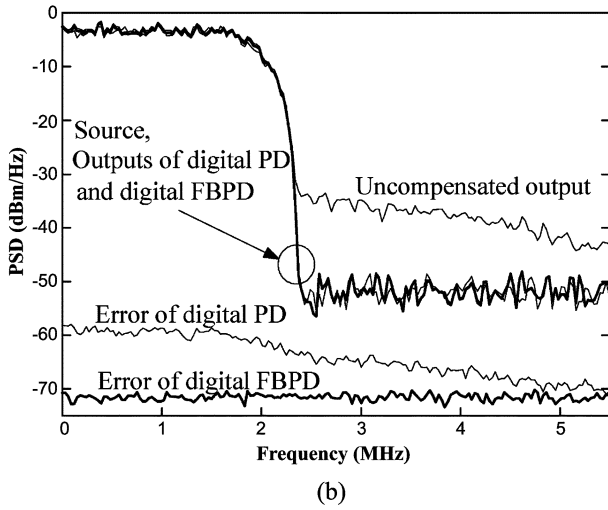
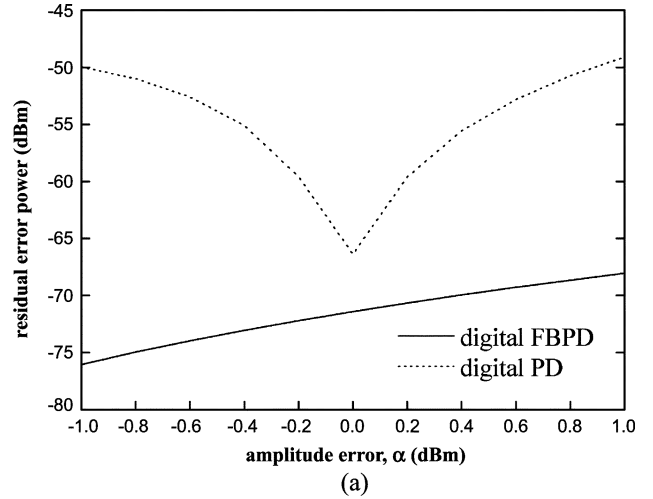
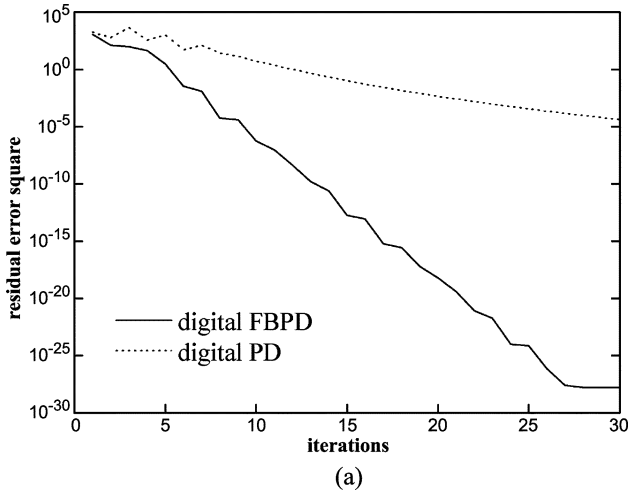


Fig. 3. (a) Comparison of the convergence behaviors. (b) PSDs of the error and output signals.

Fig. 4. Comparison of residual error powers under: (a) amplitude and (b) phase errors of predistorted input signals in analog domain (v'_d).

after convergence (DFBPD case: eight iterations, conventional case: 30 iterations). The PSD of the residual error of the DFBPD is much lower than that of DPD. These results are expected from the error cancellation mechanisms of the two PDs.

B. System Tolerance to Error

A PD linearization system is often confronted with unwanted situations such as errors from the PD signal generation, power level, or ambient temperature variations, etc. These unwanted variations reduce the cancellation level of the distortion signal. Since the DPD extracts the error signal v_e from perfect main signal cancellation for the LUT, the PD gain variations produce cancellation errors. However, the DFBPD is not affected by the unwanted gain variation due to sufficient compensation by the cancelling loop. Thus, the FBPD technique has better cancellation tolerance to error than the DPD. To check the system error tolerances of the two PDs and verify the superior system error tolerance of the proposed FBPD, we have perturbed the amplitude and phase of the predistorted signal in the analog domain (v_{d_RF} in Fig. 2), imitating the system errors; i.e., the perturbed PD input signal is expressed as

$$v'_{d_RF} = \alpha \cdot |v_{d_RF}| \angle (v_{d_RF} + \beta) \quad (13)$$

where α and β are the amplitude and phase error factors, respectively. The residual error powers versus the amplitude and phase errors are simulated, and the results are shown in Fig. 4. The residual error power is the average of final output error powers across the overall simulated band. The PD LUTs used in this simulation are fully converged to the minimum residual error. The residual error power of the DFBPD is much lower than that of the DPD at all simulated amplitude and phase error levels, and the differences of the two become larger as the error levels are increased. The results show that the DFBPD has a high cancellation error tolerance, effectively nullifying the system errors. For this simulation, the 2-dB gain variation is reduced by feedback and this tolerance can be further enhanced with stronger feedback.

C. Effect of Detector Error

As indicated earlier, the detector error affects directly the performance of the overall linearization system. However, the algorithms are different, and the linearization performance for the same detector error is different for the two cases. To investigate the responses, the linearization performance with detector errors is also simulated. The two detector error sources, the

AWGN and third-order nonlinearity, degrade the linearization performance of the DFBDP and DPD in different manners. The residual error power of the DFBDP depends linearly on the detector signal-to-noise ratio (SNR), as shown in (14), where N_{det} represents the detector noise. The residual error in the DPD with RLS algorithm is “filtered” by the gain vector K_v and multiplied by input signal v_m , as shown in (15). The residual error power of the DFBDP is given by

$$v_{a,\text{err}}(n) = \frac{G_m}{(1 - G_u) + G_m(1/G_{\text{PD}})} \cdot N_{\text{det}} \approx G_{\text{PD}}N_{\text{det}}. \quad (14)$$

The residual error power of the conventional DPD is

$$v_{a,\text{err}}(n) = G_m v_m(n) \sum_{m=0}^n K_v(m) N_{\text{det}}(m). \quad (15)$$

In the case of detector error caused by AWGN only, the residual error power of the DPD is lower than that of the DFBDP in very noisy conditions (detector SNR below 50 dB) due to the filtering effect, as shown in Fig. 5(a). However, as the detector SNR rises above 50 dB, which can be easily achieved, the linearization performance of the DFBDP improves over that of the DPD. Fig. 5(b) illustrates the residual error power as a function of the detector output third intercept point (OIP3). For the third-order nonlinearity error, the two linearization techniques show the same dependency on the error, but the FBDP has approximately 5-dB lower value. This figure shows that the error power of the final output signal is proportional to the OIP3 of the detector; i.e., the nonlinearity of the detector directly affects the linearization performance of the overall PD system. The reason for the higher level of the DPDs error power may be explained by the detector error transfer function described in (15). While the detector error from AWGN mainly affects the out-of-band signal level, the nonlinear error distorts in-band signals. Since the in-band error power is much higher than the out-of-band power and has a strong correlation with the input signal v_m , the total error power becomes higher for the DPD.

D. Effect of Modulator Error

We have simulated the linearization performance with errors of the signal modulation (up-conversion) part. AWGN and third-order nonlinearity are the modulator error sources, and the simulation method is similar to the detector error case. Fig. 6(a) shows the residual error power versus the modulator SNR. At SNR levels below 70 dB, the residual error powers of the conventional and proposed PDs are similar because they are generated mainly by noise. However, as the SNR becomes larger than 70 dB, the linearization performance of the DFBDP becomes better than that of the DPD due to the lower residual error power at convergence for DFBDP [see Fig. 3(a)]. Fig. 6(b) shows the residual error power as a function of the modulator OIP3. The nonlinearity of modulator has no effect on the linearization performance due to correction of the nonlinearity by the PD linearizer. Without any other external errors, the error power is independent of modulator OIP3, but the FBDP has superior linearity (approximately 5 dB) due to its inherently

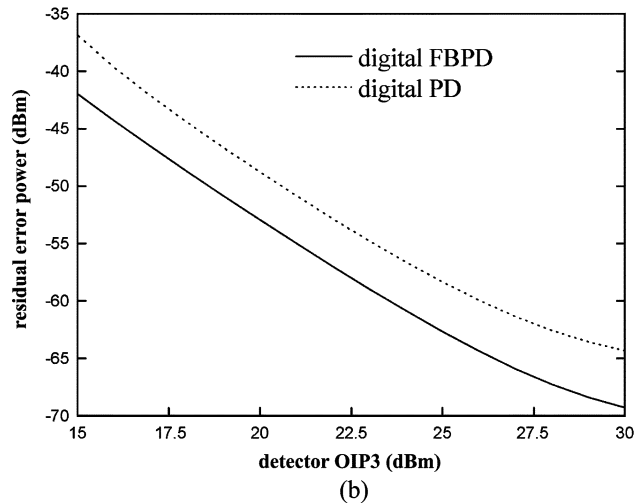
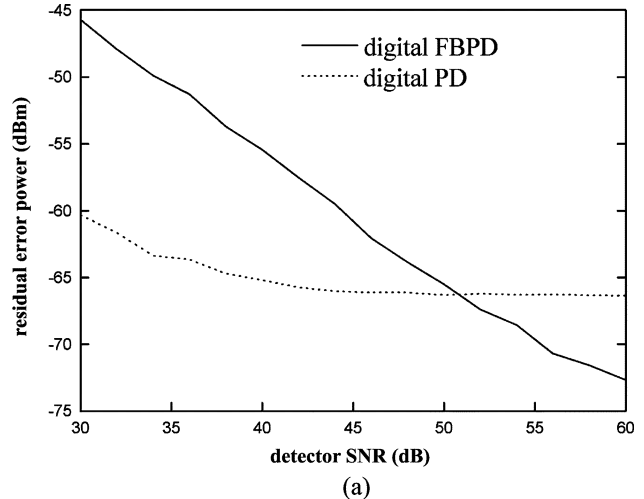


Fig. 5. Comparison of residual error power under erroneous detection conditions of: (a) AWGN and (b) third-order nonlinearity.

better linearity. In summary, the simulation results show that the proposed DFBDP has superior linearization performance in the face of modulator errors.

E. Effect of Loop Delay Mismatch

The two system diagrams represented in Fig. (2a) and (b) include additional delay blocks for the loop delay mismatch. The loop delay can be caused by RF delay mismatch in the main amplifier block, digital I/O (DAC and ADC) delay mismatch between digital and analog interface, etc. As the loop delay mismatch increases, the convergence behavior is obviously affected and finally diverges. Fig. 7 shows the convergence behaviors of the DFBDP and DPD as the delay error increases (d in Fig. 2, defined as a fraction of the sampling period). The number of iterations for convergence is smaller for the proposed PD than that for the DPD at all simulated delay errors. The DPD also diverges much earlier (at $d = 0.6$). Thus, the DFBDP has higher tolerance to loop delay mismatch.

F. Quantization Analysis

We have analyzed the effect of quantization errors of the source signal, LUT, and PD output on the linearization. If the

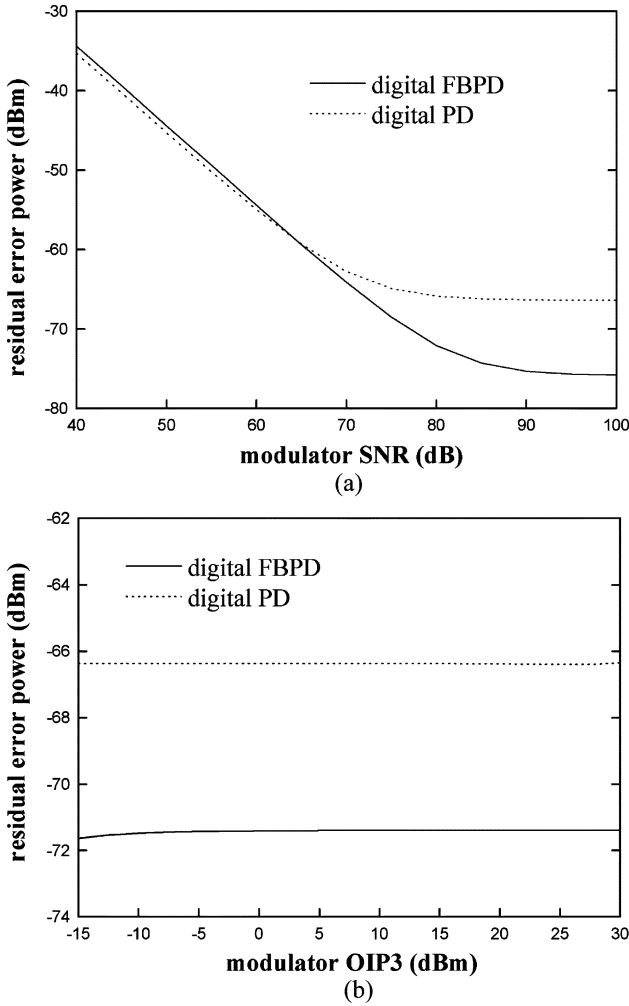


Fig. 6. Comparison of residual error power under signal modulation error conditions of: (a) AWGN and (b) third-order nonlinearity.

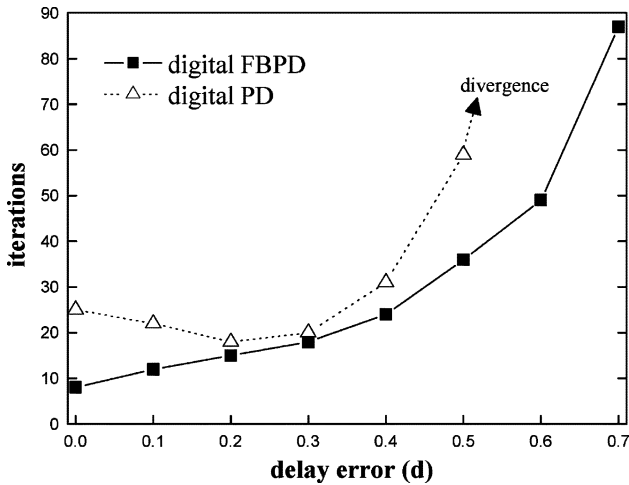


Fig. 7. Convergence behavior of the DFBDP and DPD versus delay error (d).

PD systems are ideal, i.e., the PD signal completely compensates for the amplifier distortion, the output signal of the overall

amplifier will preserve the three quantization errors. The quantization analysis is important because the optimum bit width for a given linearization performance can be determined. We have employed the quantization analysis method presented in [18] with some modifications to suit the conventional and proposed PD for WCDMA signal. The SNR and adjacent channel interference (ACI) for the quantized source signal are given by

$$\text{SNR}_{\text{in}} \approx 6.02b + 1.76 - 20 \log k \quad (\text{dB}) \quad (16)$$

$$\text{ACI}_{\text{in}} = \frac{2B_{\text{eq}}}{f_s \cdot \text{SNR}_{\text{in}}} \quad (17)$$

where b is the number of bits, k is the ratio of the peak amplitude to the rms amplitude of the signal, f_s is the sampling rate (3.84 MHz for a single-carrier WCDMA source signal), and B_{eq} is the noise bandwidth ($f_s/2$).

The average error power of the DPD by the quantized LUT is expressed as

$$\begin{aligned} \sigma_{\text{LUTi_DPD}}^2 &= \frac{(w_{k_DPD})_{\text{max}}^2}{3 \cdot 2^{2b}} \\ &\cdot \left\{ 2|v_m G|^2 + |v_m^2 w_{k_DPD} G'|^2 \right. \\ &\quad \left. + 2|v_m^3 G'| \cos[\arg(G') - \arg(G)] \right\} \quad (18) \end{aligned}$$

where G and G' are the amplifier gain and its differential value, respectively, and w_{k_DPD} is the LUT output signal, as shown in Fig. 2(a). Taking the modulation scheme into account, the total average error power in the amplifier output becomes

$$\sigma_{\text{LUT_DPD}}^2 = \int_0^1 p_m(v_m) \cdot \sigma_{\text{LUTi_DPD}}^2 dv_m \quad (19)$$

where $p_m(v_m)$ represents the probability density function (PDF) for the modulation. The SNR of the conventional PD with a quantized LUT is

$$\text{SNR}_{\text{LUT_DPD}} = \frac{\sigma_s^2}{\sigma_{\text{LUT_DPD}}^2} \quad (20)$$

where σ_s^2 is the total averaged signal power. The corresponding ACI becomes

$$\text{ACI}_{\text{LUT_DPD}} = \frac{2B_{\text{eq}}}{f_s \cdot \text{SNR}_{\text{LUT_DPD}}} \quad (21)$$

The average error power of the DFBDP with a quantized LUT is similar to the DPD, which is given by

$$\begin{aligned} \sigma_{\text{LUTi_DFBDP}}^2 &= \frac{(w_{k_DFBDP})_{\text{max}}^2}{3 \cdot 2^{2b}} \\ &\times \left\{ 2|G|^2 + |(w_{k_DFBDP} + v_m)G'|^2 \right. \\ &\quad \left. + 2|G'| \cos[\arg(G') - \arg(G)] \right\} \quad (22) \end{aligned}$$

where w_{k_DFBDP} is the LUT output signal shown in Fig. 2(b). By substituting (22) in place of (18) into (19), we obtain the total average error power $\sigma_{\text{LUT_DFBDP}}^2$, $\text{SNR}_{\text{LUT_DFBDP}}$, and $\text{ACI}_{\text{LUT_DFBDP}}$ of the DFBDP.

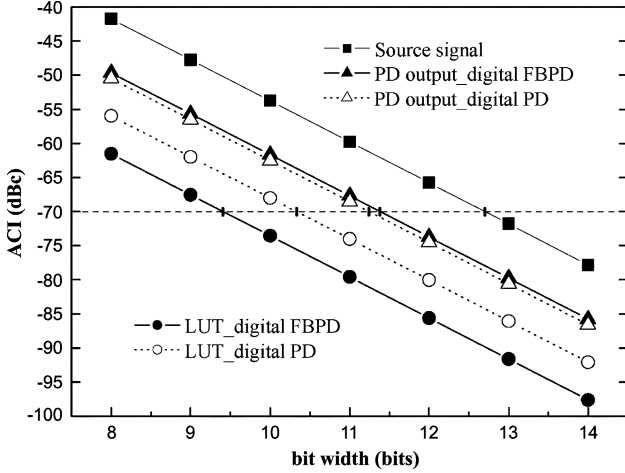


Fig. 8. ACI level of different parts with various quantization bit widths.

The ACI for the PD output is similar to that of LUT. The average error power of the DPD by the quantized output is given by

$$\sigma_{\text{PDout_DPD}}^2 = \frac{1}{3 \cdot 2^{2b}} \left\{ 2|G|^2 + |v_m^2 w_{k_DPD} G'|^2 + 2|v_m G'| \cos[\arg(G') - \arg(G)] \right\} \quad (23)$$

from which the SNR and ACI can be calculated as

$$\text{SNR}_{\text{PDout_DPD}} = \frac{\sigma_s^2}{\sigma_{\text{PDout_DPD}}^2} = \frac{\int_0^1 p_m(v_m) v_m^2 dv_m}{\int_0^1 p_m(v_m) \sigma_{\text{PDout_DPD}}^2 dv_m} \quad (24)$$

$$\text{ACI}_{\text{PDout_DPD}} = \frac{2B_{\text{eq}}}{f_s \text{SNR}_{\text{PDout_DPD}}} \quad (25)$$

The average error power of the DFBDP by the quantized PD output is given by

$$\sigma_{\text{PDout_DFBDP}}^2 = \frac{1}{3 \cdot 2^{2b}} \left\{ 2|G|^2 + |(w_{k_DFBDP} + v_m) G'|^2 + 2|G'| \cos[\arg(G') - \arg(G)] \right\} \quad (26)$$

From the average error power (26), we can also calculate the total average error power $\text{SNR}_{\text{PDout_DFBDP}}$ and $\text{ACI}_{\text{PDout_DFBDP}}$ of the DFBDP.

Fig. 8 shows ACI levels for various quantization bit widths, calculated based on the above ACI equations for the source signal, LUT, and PD output of the conventional PD and proposed PD. The ACI levels by quantization of the PD output are similar for the two PDs. For the LUT quantization, the DFBDP saves approximately 1 bit of bit width in comparison with the conventional PD for the same ACI level. Since the average error power (22) of the DFBDP does not have v_m^2 and v_m^3 terms, the LUT quantization error of the proposed FBPD is less than that of the conventional PD. Fig. 8 also shows that the bit width for the source signal is the largest. Table I presents the quantization bit widths of the source signal, LUT, and PD output required for

TABLE I
BIT WIDTHS IN THE DIFFERENT PARTS THAT RESULT IN -70 -dBc ACI CONTRIBUTION FROM EACH PART

quantization source	DFBDP	DPD
source signal	12.3 bits	12.3 bits
look-up table	9.4 bits	10.3 bits
PD output	11.4 bits	11.3 bits

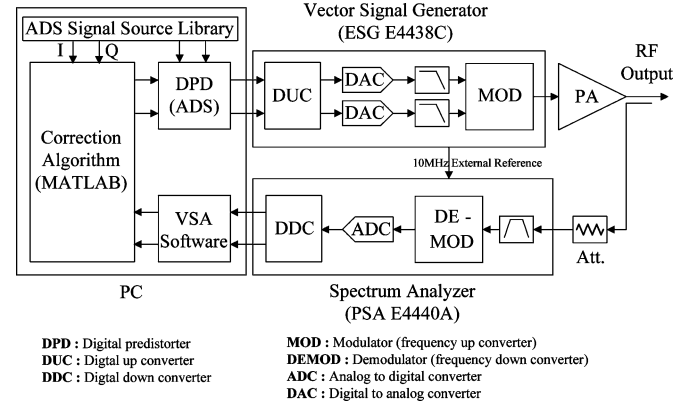


Fig. 9. Experimental setup of the DPD and FBPD.

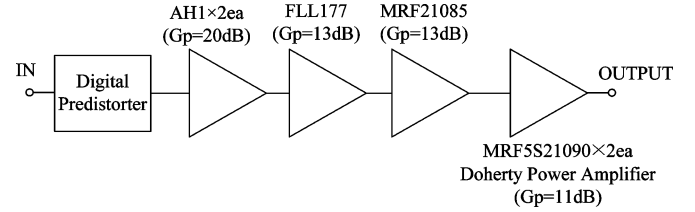


Fig. 10. DPA module used for the DPD and FBPD.

the -70 -dBc ACI level. The noise powers from the three quantizations are added up and if the bit widths given in Table I are selected, then the total ACI level is three times higher at approximately -65.23 dBc.

IV. EXPERIMENTAL RESULTS

In order to validate the proposed DFBDP technique, we have employed the ADS-ESG-VSA connected solution [19], shown in Fig. 9, as an experimental setup for quick and exact verification, and used the Doherty power amplifier (DPA) module shown in Fig. 10 with 180-W peak envelope power (PEP) and 20-W average power for a single-carrier forward-link WCDMA signal. The main amplifier of the DPA module consists of two Freescale MRF5S21090 LDMOSFETs, and the uneven power drive technique is applied to improve the performance [20]. The signal used is a 2.14-GHz forward WCDMA signal with 3.84-MHz chip rate and 9.8-dB PAR at 0.01% CCDF, generated using the 3GPP WCDMA library of ADS. The conventional DPD and proposed DFBDP have two 256-entry AM/AM and AM/PM LUTs, which are programmed by MATLAB using the RLS and FBPD algorithms, respectively.

Fig. 11 shows the adjacent channel leakage ratio (ACLR) and drain efficiency characteristics of the Doherty amplifier for the WCDMA signal. These experimental results show that the Doherty amplifier has good linearity, as well as good efficiency,

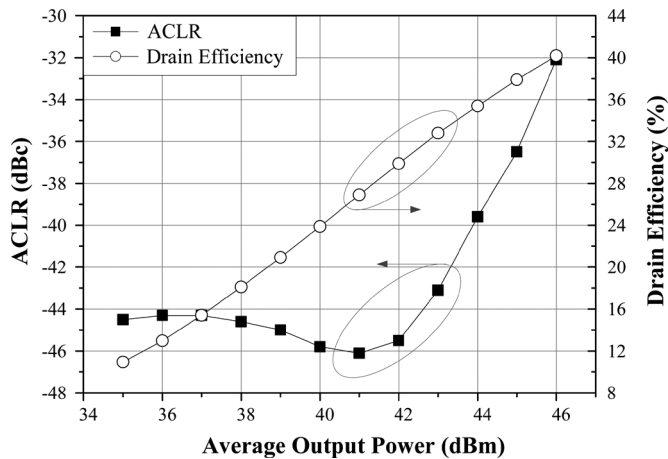


Fig. 11. Measured ACLR and drain efficiency performance of the DPA for a forward WCDMA signal.

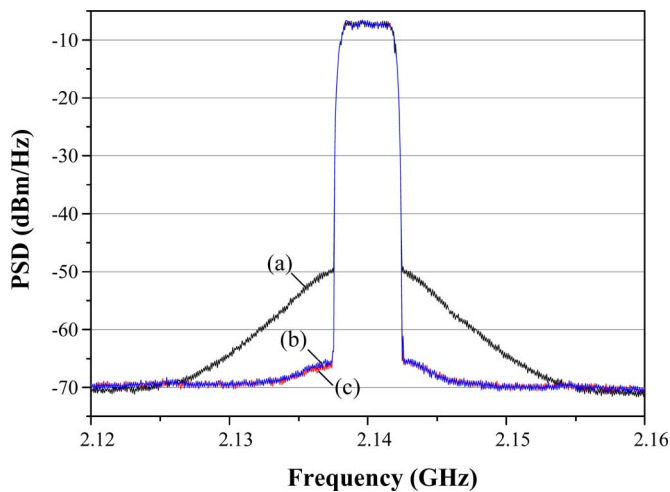


Fig. 12. Measured single-carrier WCDMA spectra before and after linearization of the DPD and FBPD at an average output power of 43 dBm. (a) Doherty amplifier without a digital predistorter. (b) Conventional digital predistorter. (c) Digital feedback predistorter.

and the amplifier is used to test the linearization performance of each digital predistortion technique. Fig. 12 shows the measured spectra before and after linearization by the DPD and FBPD for the WCDMA signal. The ACLRs at 2.5-MHz offset for the two techniques are nearly the same, i.e., -58 dBc, which is an improvement of 15 dB at an average output power of 43 dBm. These experimental results demonstrate that the both PD techniques can successfully compensate for the nonlinear characteristics of the Doherty amplifier, following the analysis described in Section III. In terms of the convergence speed, only three iterations are enough for the convergence of the DFBPD, while ten iterations are required for the conventional DPD. Furthermore, the FBPD algorithm is much simpler than the RLS algorithm of the conventional PD in terms of the complexity [see (5)–(11) and (12)], reducing the required field programmable gate array (FPGA) resources. We have not experimentally investigated all of the superior performance advantages yet (they will be reported in the near future). However, the experimental data shows that the DFBPD functions are as expected.

V. CONCLUSIONS

We have presented a new DPD concept of DFBPD. By applying a digital LUT approach for the feedback loop, the operation bandwidth limitation and oscillation problems of the analog FBPB have been solved. The DFBPD combines linearization, by DPD and feedback, and the error tolerance is significantly enhanced. To test the linearization performance of the DFBPD, we have simulated the PD and compared it to the conventional DPD for the various factors that affect the PD performance (convergence behavior, system tolerance to detector errors, modulator errors, delay mismatches, and quantization errors with various bit widths). Without any external errors, the DFBPD outperforms the DPD in convergence behavior and shows much lower residual errors. The tolerance simulation shows that the DFBPD technique is also superior compared to the DPD.

The proposed DFBPD and conventional DPD have been tested using the DPA with 180-W PEP. For a 2.14-GHz forward-link WCDMA signal, the ACLR at 2.5-MHz offset is -58 dBc for both PDs, which is an improvement of 15 dB at an average output power of 43 dBm. Only three iterations are enough for convergence of the DFBPD, while ten iterations are required for conventional DPD. Moreover, the FBPB algorithm is much simpler than the RLS algorithm of the conventional PD. Although we have not carried out extensive experimental verification, we conclude from these simulation and experimental results that the new DFBPD technique has better tolerance to error, faster convergence, and simpler structure compared to the DPD. We believe that the DFBPD will be a good candidate for the linearization of base-station transmitters.

ACKNOWLEDGMENT

The authors would like to express their gratitude to the reviewers for their comments and suggestions.

REFERENCES

- [1] S. C. Cripps, *RF Power Amplifiers for Wireless Communications*. Norwood, MA: Artech House, 1999.
- [2] P. B. Kenington, *High-Linearity RF Amplifier Design*. Norwood, MA: Artech House, 2000.
- [3] T. Nojima and T. Konno, "Cuber predistortion linearizer for relay equipment in 800 MHz band land mobile telephone system," *IEEE Trans. Veh. Technol.*, vol. VT-34, no. 6, pp. 169–177, Nov. 1985.
- [4] J. Cha, J. Yi, J. Kim, and B. Kim, "Optimum design of a predistortion RF power amplifier for multicarrier WCDMA applications," *IEEE Trans. Microw. Theory Tech.*, vol. 52, no. 2, pp. 655–663, Feb. 2004.
- [5] Y. Y. Woo, Y. Yang, J. Yi, J. Nam, J. Cha, and B. Kim, "A new adaptive feedforward amplifier for WCDMA base stations using imperfect signal cancellation," *Microw. J.*, vol. 46, no. 4, pp. 22–44, Apr. 2003.
- [6] J. K. Cavers, "Adaptation behavior of a feedforward amplifier linearizer," *IEEE Trans. Veh. Technol.*, vol. 44, no. 1, pp. 31–40, Feb. 1996.
- [7] R. J. Wilkinson and P. B. Kenington, "Specification of error amplifiers for use in feedforward transmitters," *Proc. Inst. Elect. Eng.*, vol. 139, no. 4, pt. G, pp. 477–480, Aug. 1992.
- [8] Y. Nagata, "Linear amplification techniques for digital mobile communications," in *Proc. IEEE 39th Veh. Technol. Conf.*, 1989, pp. 159–164.
- [9] K. J. Muhonen, M. Kavehrad, and R. Krishnamoorthy, "Look-up table techniques for adaptive digital predistortion: A development and comparison," *IEEE Trans. Veh. Technol.*, vol. 49, no. 9, pp. 1995–2002, Sep. 2000.
- [10] J. K. Cavers, "Amplifier linearization using a digital predistorter with fast adaptation and low memory requirements," *IEEE Trans. Veh. Technol.*, vol. 39, no. 4, pp. 374–382, Nov. 1990.

- [11] A. S. Wright and W. G. Durtler, "Experimental performance of an adaptive digital linearized power amplifier," *IEEE Trans. Veh. Technol.*, vol. 41, no. 4, pp. 395–400, Nov. 1992.
- [12] F. Antonio, W. Hamdy, P. Heidmann, J. Heizer, N. Kasturi, D. P. Osés, and C. Riddle, "A novel adaptive predistortion technique for power amplifiers," in *Proc. IEEE 49th Veh. Techno. Conf.*, May 1999, pp. 1505–1509.
- [13] M. Faulkner and M. Johansson, "Adaptive linearization using predistortion—Experimental results," *IEEE Trans. Veh. Technol.*, vol. 43, no. 2, pp. 323–332, May 1994.
- [14] S. Takabayashi, M. Orihashi, T. Matsuoka, and M. Sagawa, "Adaptive predistortion linearizer with digital quadrature modem," in *Proc. IEEE 51st Veh. Technol. Conf.*, 2000, pp. 2237–2241.
- [15] K. Horiguchi, M. Miki, J. Nagano, H. Senda, K. Yamauchi, M. Nakayama, and T. Takagi, "A UHF-band digital pre-distortion power amplifier using weight divided adaptive algorithm," in *IEEE MTT-S Int. Microw. Symp. Dig.*, 2004, pp. 2019–2022.
- [16] Y. Kim, Y. Yang, S. Kang, and B. Kim, "Linearization of 1.85 GHz amplifier using feedback predistortion loop," in *IEEE MTT-S Int. Microw. Symp. Dig.*, 1998, pp. 1675–1678.
- [17] S. Haykin, *Adaptive Filter Theory*, 4th ed. Upper Saddle River, NJ: Prentice-Hall, 2001.
- [18] L. Sundström, M. Faulkner, and M. Johansson, "Quantization analysis and design of a digital predistortion linearizer for RF power amplifiers," *IEEE Trans. Veh. Technol.*, vol. 45, no. 4, pp. 707–719, Nov. 1996.
- [19] "Connected simulation and test solutions using the Advanced Design System," Agilent Technol., Palo Alto, CA, Applicat. Note 1394, 2000.
- [20] J. Kim, J. Cha, I. Kim, and B. Kim, "Optimum operation of asymmetrical-cells-based linear Doherty power amplifiers—Uneven power drive and power matching," *IEEE Trans. Microw. Theory Tech.*, vol. 53, no. 5, pp. 1802–1809, May 2005.



Young Yun Woo received the B.S. degree in electrical and computer engineering from Han-Yang University, Seoul, Korea, in 2000, and the Ph.D. degree in electrical engineering from the Pohang University of Science and Technology (POSTECH), Pohang, Gyeongbuk, Korea, in 2007.

In 2007, he joined the Samsung Electronics Company Ltd., Suwon, Gyeonggi, Korea. His current research interests include RF PA design, linear power amplifier (LPA) system design, and DPD techniques for linearizing high PAs.



Jangheon Kim received the B.S. degree in electronics and information engineering from Chon-buk National University, Chonju, Korea, in 2003, and is currently working toward Ph.D. degree at the Pohang University of Science and Technology (POSTECH), Pohang, Gyeongbuk, Korea.

His current research interests include highly linear and efficient RF PA design, memory effect compensation techniques, and linearization techniques.



Jaehyok Yi received the M.S. and Ph.D. degrees in electrical engineering from the Pohang University of Science and Technology (POSTECH), Pohang, Gyeongbuk, Korea, in 1999 and 2005, respectively.

In 2005, he joined the LG Electronics Company Ltd., Seoul, Korea. His research interests include the design and simulation of the behavior of linear RF PAs and linearization techniques.



Sungchul Hong received the B.S. degree in electrical and electronic engineering from Yonsei University, Seoul, Korea, in 2003, and the Master degree in electrical engineering from the Pohang University of Science and Technology (POSTECH), Pohang, Gyeongbuk, Korea, in 2007.

In 2007, he joined the Samsung Electronics Company Ltd., Suwon, Gyeonggi, Korea. His research interests include design of PAs, DPD techniques, and highly efficient transmitter systems.



Ildu Kim received the B.S. degree in electronics and information engineering from Chon-nam National University, Kwangju, Korea, in 2004, and is currently working toward Ph.D. degree at the Pohang University of Science and Technology (POSTECH), Pohang, Gyeongbuk, Korea.

His current research interests include RF PA design and linearity and efficiency improvement techniques.



Junghwan Moon received the B.S. degree in electrical and computer engineering from the University of Seoul, Seoul, Korea, in 2006, and is currently working toward the Ph.D. degree at the Pohang University of Science and Technology (POSTECH), Pohang, Gyeongbuk, Korea.

His current research interests include highly linear and efficient RF PA design.



Bumman Kim (M'78–SM'97–F'07) received the Ph.D. degree in electrical engineering from Carnegie–Mellon University, Pittsburgh, PA, in 1979.

From 1978 to 1981, he was engaged in fiber-optic network component research with GTE Laboratories Inc. In 1981, he joined the Central Research Laboratories, Texas Instruments Incorporated, where he was involved in development of GaAs power field-effect transistors (FETs) and monolithic microwave integrated circuits (MMICs). He has developed a large-signal model of a power FET, dual-gate FETs for gain control, high-power distributed amplifiers, and various millimeter-wave MMICs. In 1989, he joined the Pohang University of Science and Technology (POSTECH), Pohang, Gyeongbuk, Korea, where he is a Namko Professor with the Department of Electrical Engineering, and Director of the Microwave Application Research Center, where he is involved in device and circuit technology for RF integrated circuits (RFICs). In 2001, he was a Visiting Professor of electrical engineering with the California Institute of Technology, Pasadena. He has authored over 200 technical papers.

Dr. Kim is a member of the Korean Academy of Science and Technology and the Academy of Engineering of Korea. He was an associate editor for the IEEE TRANSACTIONS ON MICROWAVE THEORY AND TECHNIQUES and a Distinguished Lecturer of the IEEE Microwave Theory and Techniques Society (IEEE MTT-S).